Hippocampal and visuospatial learning defects in mice with a deletion of frizzled 9, a gene in the Williams syndrome deletion interval

Chunjie Zhao[1,*,†], Carmen Avilés[1], Regina A. Abel[3], C. Robert Almli[3], Patrick McQuillen[2] and Samuel J. Pleasure[1,†]

[1]Department of Neurology, Graduate Programs in Neuroscience, Developmental Biology and Biomedical Sciences, Room S-268, 513 Parnassus Avenue, University of California, San Francisco, CA 94143, USA
[2]Department of Pediatrics, University of California, San Francisco, CA 94143, USA
[3]Departments of Neurology, Psychology, Developmental Neuropsychobiology Laboratory, Programs in Occupational Therapy, Neuroscience, Washington University Medical School, St Louis, MO 63108, USA

*Present address: Genetics Research Center, Southeast University Medical School, State Education Ministry Laboratory of Developmental Genes and Human Diseases, 87 Dingjiaqiao Road, Nanjing, Jiangsu Province, 210009, PR China

†Authors for correspondence (e-mail: zhaocj@seu.edu.cn or samuelp@itsa.ucsf.edu)

Accepted 15 April 2005

Development 132, 2917-2927
Published by The Company of Biologists 2005
doi:10.1242/dev.01871

Summary

Wnt signaling regulates hippocampal development but little is known about the functions of specific Wnt receptors in this structure. Frizzled 9 is selectively expressed in the hippocampus and is one of about 20 genes typically deleted in Williams syndrome. Since Williams syndrome is associated with severe visuospatial processing defects, we generated a targeted null allele for frizzled 9 to examine its role in hippocampal development. Frizzled 9-null mice had generally normal gross anatomical hippocampal organization but showed large increases in apoptotic cell death in the developing dentate gyrus. This increase in programmed cell death commenced with the onset of dentate gyrus development and persisted into the first postnatal week of life. There was also a perhaps compensatory increase in the number of dividing precursors in the dentate gyrus, which may have been a compensatory response to the increased cell death. These changes in the mutants resulted in a moderate decrease in the number of adult dentate granule cells in null mice and an increase in the number of hilar mossy cells. Heterozygous mice (the same frizzled 9 genotype as Williams syndrome patients) were intermediate between wild type and null mice for all developmental neuronanatomic defects. All mice with a mutant allele had diminished seizure thresholds, and frizzled 9 null mice had severe deficits on tests of visuospatial learning/memory. We conclude that frizzled 9 is a critical determinant of hippocampal development and is very likely to be a contributing factor to the neurodevelopmental and behavioral phenotype of patients with Williams syndrome.

Key words: Wnt, Dentate gyrus, Epilepsy, Mossy cell, Apoptosis

Introduction

Wnts regulate the development of dorsal structures (including the hippocampus) in the developing mammalian central nervous system (Muroyama et al., 2002). Gain-of-function studies, examining the brains of mice overexpressing a dominant-active version of the Wnt effector molecule β-catenin in the cerebral cortex, support a role for the canonical Wnt pathway in regulating neural precursor proliferation during the early stages of development (Chenn and Walsh, 2002). Loss-of-function studies, examining mice with mutations in Wnt3a, Lef1 and Lrp6, show that canonical Wnt signaling is particularly critical in the developing hippocampus and dentate gyrus (Lee et al., 2000; Galceran et al., 2000; Zhou et al., 2004). What has not been clear to date is the identity of the receptors utilized for Wnt signaling in the developing hippocampus. We recently showed that Lrp6, a Wnt co-receptor required for the canonical Wnt pathway, is required for some aspects of Wnt effects in the hippocampus (Zhou et al., 2004) but the identities of other receptor components are not clear. Recent studies have examined the phenotype of mutants in one class of Wnt receptors, the frizzled (Fzd) genes, and found that they are involved in a variety of phenotypes in the developing brain, including regional neurotrophic functions and regulation of major fiber tracts (Wang et al., 2001; Wang et al., 2002). So far, none of the frizzled mutants have phenocopied any of the Wnt ligand mutants. This may be due to the extensive expected redundancy among the 10 frizzled family members due to considerable sequence similarity and overlap in expression patterns (Wang et al., 1996; Kim et al., 2001).

We have focused on the function of frizzled 9 because of its selective expression pattern in the hippocampus throughout life (Kim et al., 2001; Zhao and Pleasure, 2004). Previous studies demonstrated that frizzled 9 may act as a Wnt receptor in the canonical Wnt pathway, signaling via β-catenin (Karasawa et al., 2002). A further role for frizzled 9 in brain development is suggested by the fact that frizzled 9 is within the Chr. 7q11

deletion interval for Williams syndrome, a neurodevelopmental cognitive disorder in humans (Wang et al., 1997; Wang et al., 1999). Williams syndrome patients have a characteristic cognitive profile that includes sparing of language and social function but severe involvement of spatial cognitive processing and memory (cognitive processes dependent on hippocampal function), with sparing of language and social functions (Bellugi et al., 1999). Here we present evidence that frizzled 9 null and heterozygous mutants have increased apoptotic cell death and increased precursor proliferation during hippocampal development, and that null mutants have severe defects in learning and memory reflecting hippocampal functional deficits that may be reminiscent of Williams syndrome.

Materials and methods

Targeted disruption of frizzled 9

A mouse frizzled 9 genomic clone was obtained from a 129SvJ library. The entire 1.8 kb frizzled 9 coding region was replaced by an ires-Lacz-LoxpPGKneoLoxp selection cassette, and the electroporation was performed using standard procedures. Homologous recombinant clones were identified by Southern blot. The targeted ES clones were injected into C57BL/6J blastocysts and chimeric mice were bred with C57BL/6J females. Frizzled 9 mutants were obtained from heterozygous intercrosses. Genotyping was carried out using tail DNA by PCR amplification. The wild-type frizzled 9 allele was detected using primers 5′-CAGTCTG-TGAGTTGGTCCCCAG-3′ and 5′-GCCCCTACCCACCCATACT-TTG-3′. The neo transgene was amplified using primers 5′-TG-GGCACAACAGACAATCGG-3′ and 5′-ACTTCGCCCAATAGC-AGCCAG-3′. All animal studies were performed according to approved protocols by the University of California, San Francisco. The animals used in this study were F3-F7 generations of backcross into the C57Bl/6 background and in each case littermates (that should be balanced for potential genetic background factors) were used for controls. All the behavioral testing was performed in animals at the F7 generation.

Immunohistochemistry and semiquantitative cell counting in developing brains

Brains were either immersed (embryonic brains) into or perfused (older than P0) by freshly prepared 4% PFA, cryoprotected in 30% sucrose, embedded in OCT and sectioned at 14 μm (embryonic brains) or 40 μm (older than P8) on a cryostat or sliding microtome. Sections were permeabilized by 0.1% Triton-X100 in PBS, blocked in 20% lamb serum and incubated with primary antibodies overnight at 4°C, then with either biotinylated secondary antibodies that were viewed by the ABC method with diaminobenzidine (DAB) or fluorescence conjugated secondary antibodies. Antibodies and reagents used were: rabbit anti-frizzled 9 antiserum produced using the COOH-terminal peptide sequence CHYKAPTVVLHMTKTDPSLENPTHL; rabbit anti-prox1 (Bagri et al., 2002); rabbit anti-phospho-Histone H3: Upstate, cat#06-570; rabbit anti-Calretinin (Chemicon, cat#AB5054); rabbit anti-Calbindin (Chemicon); rabbit anti-GFAP (Chemicon); AlexaFluor 594 goat anti-mouse IgG (Molecular Probes, A11005), Alexafluor 488 goat anti-rabbit IgG (Molecular Probes, A11008), Biotinylated goat anti-mouse IgG (Vector Laboratories, BA2000), Biotinylated goat anti-rabbit IgG (Vector Laboratories, BA1000). VECTASTAIN ABC kit: Vector Laboratories, pk-6100. 3, 3′-diaminobenzidine (DAB): Sigma, D-5637.

For counting anti-Phospho-Histone H3- or BrdU-labeled cells in developing brains, six sections at the same coronal level were chosen for each animal, labeled cells in the medial and lateral cortical wall at E14.5, in dentate gyrus at E18.5 and P8. Anti-Phospho-Histone H3-labeled cells in adult brains were counted using the same methodology as for the stereologic analysis (see below). For hilar mossy cell counts, brains were cut at 50 μm from anterior to posterior and one of every eight sections were chosen for counting. Three independent pairs of littermates at each age were quantified and the data was analyzed by Student's *t*-test.

To examine whether there was compensatory gliosis or mossy fiber sprouting due to the alterations in dentate structure, we used antibodies to GFAP (Chemicon) and to Calbindin (Chemicon) to qualitatively examine wild type, heterozygous and homozygous mutant mice. Immunohistochemistry was performed as described above.

Stereologic analysis of adult dentate granule and hippocampal pyramidal cell number and layer volume

An investigator blind to frizzled 9 genotype performed quantitative stereologic analysis of cell number and layer volume in dentate and hippocampus using nissl stain to identify all cells. Adult mice (all about 12 weeks old) from each genotype (wild type, heterozygous and homozygous, n=5-7 per genotype) were sectioned at 40 μm (nissl) or 50 μm (immunohistochemistry) in the coronal plane throughout the extent of hippocampus. A series of every tenth section was randomly selected and processed for nissl stain immunocytochemistry. Total cell number was estimated using the optical fractionator method (West et al., 1991) and Stereo Investigator software (Microbrightfield, Inc., Williston, VT). Using accepted anatomic boundaries (The Rat Brain, Paxinos and Watson), the relevant structure was traced at low power (4×) using the live image generated with a Nikon Eclipse 600 microscope and a digital video camera. Pilot studies determined the dissector dimensions (Table 1) to count approximately one cell per sampling frame and allowing for a guard zone above and below the sampling site. A 60× immersion oil, 1.4 numerical aperture objective was used to achieve optimal optical sectioning during stereologic analysis. The Stereo Investigator software placed dissector frames using a systematic-random sampling design within each contour. Only 'caps' were counted, defined as immunoreactive or nissl stained somata that came into focus while focusing down through the dissector height. Adequate sampling was confirmed by coefficients of error for cell number less than 0.05 (Table 1). Dentate granule and hippocampal pyramidal cell layer volume estimates were calculated using the Cavalieri principle and contours traced at low power.

TUNEL staining and cell counting

Brains were fixed as described as above, then dehydrated through ethanol, embedded in paraffin and serially sectioned at 10 μm on a conventional microtome. Sections were deparaffinized and refixed by 4% PFA, followed by treatment of 20 μg ml^{-1} proteinase K for 30 minutes at room temperature. After washing out proteinase K, sections were refixed and incubated with biotinylated nucleotide mix and TdT enzyme (Promega, G7130) at 37°C for 1 hour. The reaction was then stopped by 2×SSC. Sections were washed by PBS, immersed in 0.3% hydrogen peroxide for 3 minutes to block the endogenous peroxidases, and incubated with streptavidin HRP for 30 minutes at room temperature and detected by DAB staining. 15 serial sections at the same coronal level for each animal were chosen for counting. Labeled cells/clusters in the medial wall at E14.5, in dentate gyrus and fimbria at E18.5 and dentate gyrus at P8 were counted. Three independent sets of littermates at each age were quantified and the data was analyzed by Student's *t*-test.

Brdu injection and detection

Mice were injected with 50 μg Brdu g^{-1} body weight and sacrificed 2 hours later. Cryostat sections were prepared as described above and treated with 2N HCl for 30 minutes at 37°C, neutralized with 0.1 M borate buffer pH 8.5 for 15 minutes, washed with PBS-0.1% Triton-X100. After blocking in 20% lamb serum, sections were incubated with anti-Brdu antibody (Roche, cat#1170376) overnight at 4°C, then

Table 1. Parameters of stereology in adult hippocampus

Region	Stain	Dissector dimensions (x:y:z μm)	Sampling grid (x:y μm)	CE (mean±s.d.)
Dentate granule layer	Nissl	11:11:6	150:150	0.04±0.004
Hippocampal pyramidal layer	Nissl	25:25:6	300:300	0.05±0.006

detected by AlexaFluor 594 goat anti-mouse IgG (Molecular Probes, A11005) or with the ABC method.

RT-PCR

P0 mouse brains were dissected in cold DEPC treated PBS, flash-frozen in dry ice, quickly weighed and immediately homogenized in lysis buffer provided in the Absolutely RNA RT-PCR Miniprep Kit (Strategene, cat#400800), and isolation of RNA was performed by following the instructions provided by the manufacturer. cDNA was synthesized at 45°C for 20 minutes and pre-denatured at 95°C for 2 minutes. PCR was performed by the following primer sets: 5′-CCT-GCCAGCACTCAAAACTATCG-3′ and 5′-GCACTGTGTAAAG-GATGGAAAAGACTCC-3′ for amplification of frizzled 9; 5′-TAA-CCGTCACGAGCATCATCCTC-3′ and 5′-CCAGGTAGCGAAA-GCCATTTTTTG-3′ for *LacZ*. The conditions were 40 cycles of de-naturation at 95°C for 30 seconds, annealing at 65°C for 30 seconds, extension at 72°C for 30 seconds, then followed by a final extension at 72°C for 10 minutes using SuperScript One-Step RT-PCR kit (Invitrogen, cat#10928-034). PCR products were analyzed in a 2% agarose gel.

Seizure induction

Ten-month-old frizzled 9 mutants, heterozygotes and their wild-type littermates were injected with pentylenetetrazole (Sigma, p-6500) i.p. at 40 μg g^{-1} body weight. The mice were observed for the latency to first twitch and to tonic-clonic (T-C) seizure after injection. The data were analyzed by Student's *t*-test.

Analysis of visuospatial learning and memory

The mice were transferred from the University of California, San Francisco to the Developmental Neuropsychobiology Laboratory (Director: C. Robert Almli) at Washington University School of Medicine (St Louis, MO, USA) at 10 days prior to the onset of behavioral testing. Subjects used for behavioral testing were 29 adult (120 days of age) male frizzled 9 mice: –/– (n=9), +/– (n=12), +/+ (n=8). Mice were housed under a 12:12 hour light:dark cycle, with food and water freely available throughout the study.

Spatial learning and memory was assessed in the Morris water maze (Morris, 1984). The water maze and the testing procedures were described in detail previously (Almli et al., 2000; Altemus and Almli, 1997). Briefly, a tub scaled specifically for mice (diameter=92 cm) was filled with water (21±1°C) made opaque with nontoxic, white tempera paint. The four walls of the maze room were differentially decorated with visually distinct designs.

Each mouse was tested in each of three maze testing conditions (in the following order): Place Condition (spatial condition) – the escape platform was hidden (submerged 1 cm below surface of the water) in a fixed location of a specific maze quadrant for each acquisition (learning) trial; Random Condition (unsolvable control condition) – the escape platform was hidden (submerged 1 cm below surface of the water) in a randomly selected quadrant for each acquisition (learning) trial; Cue Condition (vision and motor ability control condition) – the escape platform was visible (elevated 1 cm above the surface of the water) in a fixed location of a specific maze quadrant for each acquisition (learning) trial. The mice were 'rested' for two weeks between testing on the place and random testing conditions, and between testing on the random and cue testing conditions, i.e. a 2 week 'time-out' interval between testing conditions to reduce carry-over effects. This procedure was validated during extensive preliminary work with rats and mice.

During testing on the place, random and cue conditions, the mice were given six 1 minute acquisition (learning) trials per day for the consecutive 6 days. For each acquisition trial, the mouse was held against the wall of the maze in the center of a semi-randomly assigned quadrant not containing the escape platform. Time to escape to the platform (escape latency) was determined using Videomex-One Image Motion System and Water Maze Monitoring software (Columbus Instruments, Columbus, Ohio). After completion of the six acquisition trials each day, the platform was removed from the maze, and a single, 1 minute probe (memory) trial was performed. The total time that the mouse spent in quadrant that had previously contained the escape platform was measured as probe time (for testing under the random condition, a specific quadrant was arbitrarily designated as the 'probe/platform' quadrant). In addition, the number of times that the mouse crossed the exact spot/position where the platform had be located during acquisition trials was measured as annulus crossings. Data analyses were performed with Statistica (Statsoft, Corp.), with alpha at P<0.05. Analysis of variance (ANOVA) with Tukey's HSD and Newman-Keuls post-tests were used.

Results

Generation of frizzled 9 mutant mice

We developed an antiserum specific for frizzled 9 and found that the protein was distributed in the entire medial wall of the cortex (from which the hippocampus arises) at mid-gestation, and that there was substantial expression throughout the hippocampus, including hilar mossy cells at later stages (Zhao and Pleasure, 2004; Zhao and Pleasure, 2005). Further studies showed that frizzled 9 was also expressed in dividing precursors in the dentate gyrus. Cells double-labeled with BrdU administered acutely prior to sacrifice were included among cells expressing the highest levels of frizzled 9 at E18.5 (Zhao and Pleasure, 2005). This indicated that at this developmental stage, actively proliferating dentate precursors expressed frizzled 9. To assess the functional significance of frizzled 9 during hippocampal development, we targeted the frizzled 9 gene using homologous recombination to delete the entire single frizzled 9 coding exon (Fig. 1A,B shows the targeting strategy and a Southern blot showing a targeted cell line). To confirm that the targeted mice are frizzled 9 nulls we isolated brain RNA from +/+, +/– and –/– mice and performed RT-PCR using primers specific for either *LacZ* (which is driven by the endogenous frizzled 9 promoter in the targeted allele) or frizzled 9. This analysis showed only *LacZ* mRNA expression in –/– animals, *LacZ* expression and frizzled 9 expression in +/– animals and only frizzled 9 expression in +/+ animals (Fig. 1C). Unfortunately although *LacZ* mRNA was detectable by PCR, X-gal staining in heterozygous or null animals was not detectable for unclear reasons. Frizzled 9 +/+, +/– and –/– animals were present in the expected Mendelian frequency as neonates and at adulthood and mutant animals were fertile. Immunohistochemistry with our frizzled 9 antiserum also confirmed the absence of frizzled 9 protein in

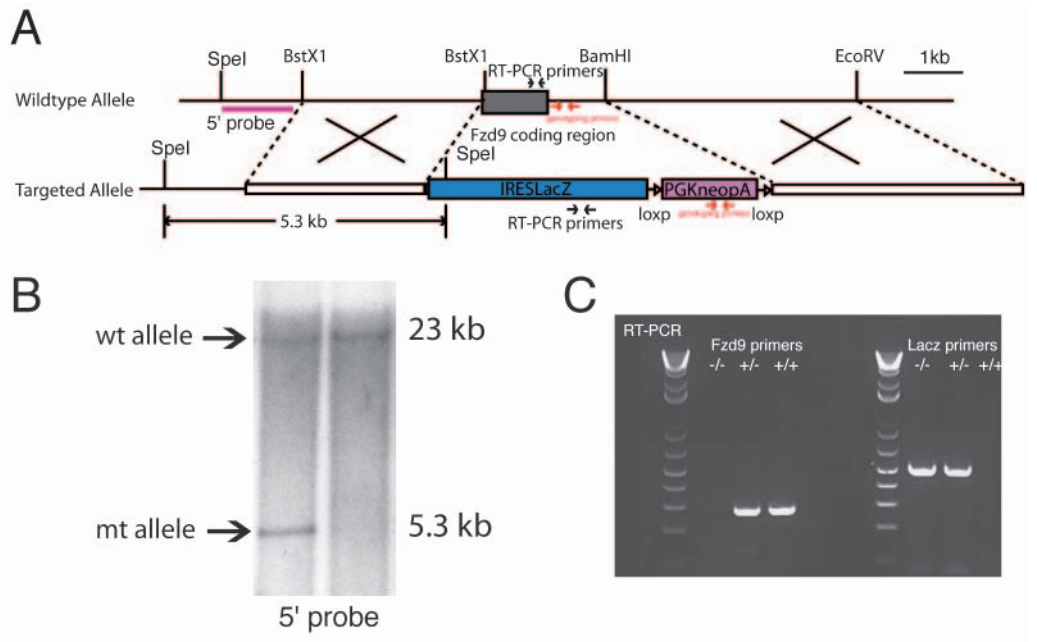

Fig. 1. Targeting the frizzled 9 allele. (A) Targeting strategy to generate the frizzled 9 null allele. The location of the genotyping primers and Southern probe are shown. (B) Southern blot showing the targeted allele. (C) RT-PCR for frizzled 9 and *LacZ* in mutant mice.

the –/– mice and an intermediate level of expression in +/– mice (data not shown). Therefore, we conclude that our frizzled 9 mutant mice were null for frizzled 9 and that heterozygous mice had intermediate expression.

We performed routine histology using hematoxylin/eosin staining to evaluate overall brain organization during development and adulthood in mutant mice. At E14.5, overall organization of the cortex in the coronal plane showed no significant alterations in brain structure (data not shown). In adulthood the overall cytologic organization of the neocortex, limbic cortex and hippocampus were also unchanged (data not shown). Since frizzled 9 was most abundantly expressed in the dentate gyrus by late gestation, we examined dentate granule cell layer organization at several developmental stages (data not shown) and in adults using an antibody to Prox1, a specific granule cell marker (Bagri et al., 2002). This also showed no obvious alterations in structure (data not shown).

Increased proliferation in the medial cortical wall and dentate gyrus

Previous studies have implicated Wnt signaling in regulating precursor proliferation in the dorsal spinal cord and medial cortical wall (Ikeya et al., 1997; Alder et al., 1999; Lee et al., 2000). These studies predict that, if frizzled 9 is required for canonical Wnt/β-catenin signaling, then precursor proliferation should be decreased in the medial cortical wall of mutant mice. Surprisingly, when we examined the medial cortical wall of mutants we instead noted a small increase in precursor proliferation at E14.5 (Fig. 2A,B). We quantified this data and found that there was a statistically significant increase in the number of M-phase precursor cells in the medial cortical wall of –/– mice and an intermediate change in +/– mice (still statistically significant when compared to +/+ mice) (Fig. 2B), while the number of M-Phase precursors in the lateral cortical wall, where frizzled 9 is very weakly expressed, showed no change according to genotype (Fig. 2A,B).

By E18.5 proliferating dentate granule precursors have migrated to the dentate hilus to form a displaced proliferative zone (Bagri et al., 2002). At this age, we also saw a statistically significant increase in M-Phase precursors in the dentate gyrus (Fig. 2A,B). By P8 and in adulthood we no longer saw any difference according to genotype (Fig. 2A,B). Thus, frizzled 9 mutant mice had a small developmental increase in the number of dividing precursor cells.

Although labeling of M-Phase cells with Phospho-Histone-H3 antibody has two advantages over BrdU labeling for counting acutely dividing precursors (these are the exclusion of potential teratogenic effects of BrdU and the decreased variability based on potential injection errors), acute BrdU labeling is the more established methodology. To determine if our approach of counting M-Phase cells was reliable to document the magnitude differences we observed, we also counted BrdU labeled after acute injection of BrdU at E18.5 and found the same magnitude difference based on genotype (Fig. 2C).

Since most granule cells are born postnatally (Altman and Das, 1965a; Altman and Das, 1965b), it seemed possible that the small increase in precursor cell numbers would lead to a more dramatic change in granule cell number by adulthood despite the overall normal organization of the dentate granule cell layer. To address this question in 12-week old mice we used unbiased stereologic techniques to count the total number of dentate granule cells and the total dentate volume in all three genotypes. Unexpectedly this analysis showed that there was a statistically significant approximately 20% decrease in the number of dentate granule cells in mutant mice (Fig. 3A,B). At the same time, we found no changes in the pyramidal cell number of volume of the pyramidal cell fields using stereologic methods (Fig. 3B).

Cell death is elevated in the dentate gyrus of frizzled 9 mutant mice

How can increased numbers of precursors lead to a decreased number of dentate granule neurons? If there is a consistent increase in precursor number throughout development this should translate into a substantial increase in neurons by adulthood. This suggested the possibility that some other cellular process might be perturbed in the mutant mice. To explain this conundrum we examined programmed cell death, using TUNEL staining, in dentate development. We reasoned that the small increase in precursor number might be partial

compensation for a more substantial alteration in cell death.

By E14.5 the dentate anlage was a site of fairly abundant TUNEL+ nuclei in wild-type mice. At low power, these cells were consistently present in 1-2 clusters each consisting of 1-4 cells when examined at higher power (Fig. 4A,B). In mutant –/– mice there was dramatic (more than five-fold) increase both in the number of clusters and the number of cells per cluster (Fig. 4A,B). Frizzled 9+/– mice were intermediate in both the number of clusters and number of TUNEL+ cells (Fig. 4A,B). The differences between genotypes both in clusters of dying cells and the total number of dying cells were all statistically significant. We also examined the medial cortical wall before the dentate gyrus begins to form (at E12.5, when frizzled 9 protein is very weakly expressed) and found no change in dying cells in the region of the future dentate (the neuroepithelium immediately dorsal to the cortical hem) and cortical hem (Fig. 4A). This region was previously noted to be a hotspot for developmental apoptosis under the control of BMP signaling (Furuta et al., 1997; Hebert et al., 2002; Panchision et al., 2001) but was not altered in frizzled 9 mutants.

Later in gestation both the dentate hilus, containing the bulk of the ongoing proliferating dentate precursors, and the fimbria continued to be areas with substantial numbers TUNEL+ cells in wild-type mice. At this age the fimbria marked the boundary of the still prominent migratory route for granule neurons and precursors (Bagri et al., 2002). Again there was an almost three-fold increase in TUNEL+ cells in the dentate and fimbria of frizzled 9 null animals and an intermediate increase in heterozygotes (Fig. 4A,B). At P8, when the displaced dentate proliferative zone was still active, there was a smaller but still statistically significant increase in TUNEL+ cells in nulls but not heterozygotes (Fig. 4A,B). In adults we detected no alteration dependent on genotype, however the very low level of apoptosis at these later ages may have made differences difficult to discern (data not shown).

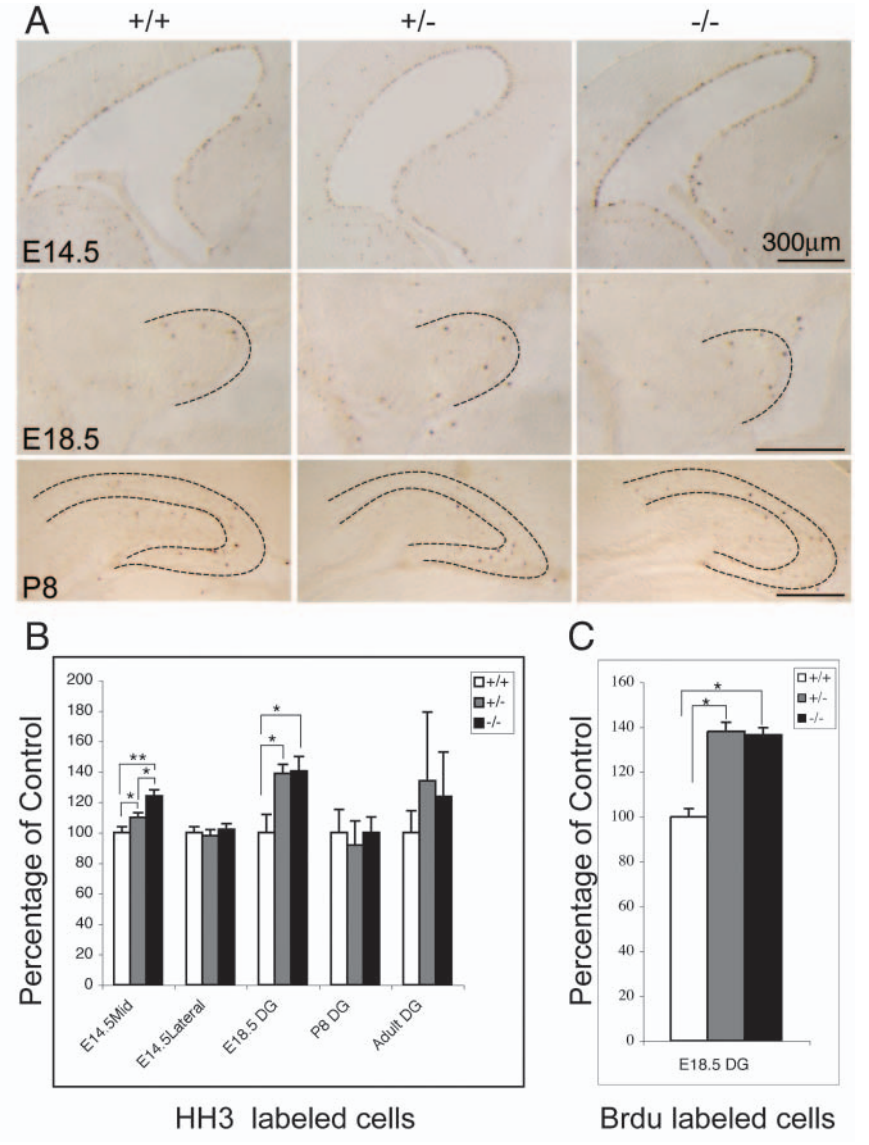

Fig. 2. Precursor proliferation in the brains of frizzled 9 mutants. (A) Phospho-Histone-H3 is a marker of M-Phase of the cell cycle. Shown are examples of staining from brains at E14.5, E18.5 and P8. (B) Semi-quantitative analysis of the numbers of M-Phase cells showing significant increases in the medial cortical wall of mutant mice at E14.5 and in the dentate gyrus of E18.5 mutants but not P8 or adults. (C) Similar analysis of the numbers of BrdU labeled nuclei after acute BrdU administration at E18.5. **P*<0.05; ***P*<0.005.

Mutants had increased numbers of hilar mossy cells

One of the other important hilar neuronal populations are the mossy cells. These excitatory neurons are one of the chief synaptic targets of the granule cells and their participation in the hippocampal circuit has been postulated to be crucial in the etiology of temporal lobe epilepsy in humans (Ratzliff et al., 2002; Sloviter et al., 2003). We also noted quite prominent expression of frizzled 9 in this other population of dentate neurons (Zhao and Pleasure, 2004; Zhao and Pleasure, 2005), so we examined their numbers as well. Interestingly we found a dramatic increase in mossy cell number leading to substantially increased neuronal density in the hilus (Fig. 5). Previous anatomic studies showed that these neurons originate from the germinative zone immediately adjacent to the primordial dentate granule ventricular zone (Nowakowski and Rakic, 1981; Nowakowski and Rakic, 1979), thus it seems likely that the increase in precursor proliferation in the ventricular zone at mid-gestation included the cells generating mossy cells. Thus, the loss of frizzled 9 led to reduction in the total numbers of granule cells but increased mossy cells. This raised the possibility that there might be functional, behavioral defects in the frizzled 9 mutant mice.

Lowered seizure threshold in frizzled 9 mutant mice

One sensitive measure of integrity of the hippocampal circuitry is the level of excitability in response to chemoconvulsants

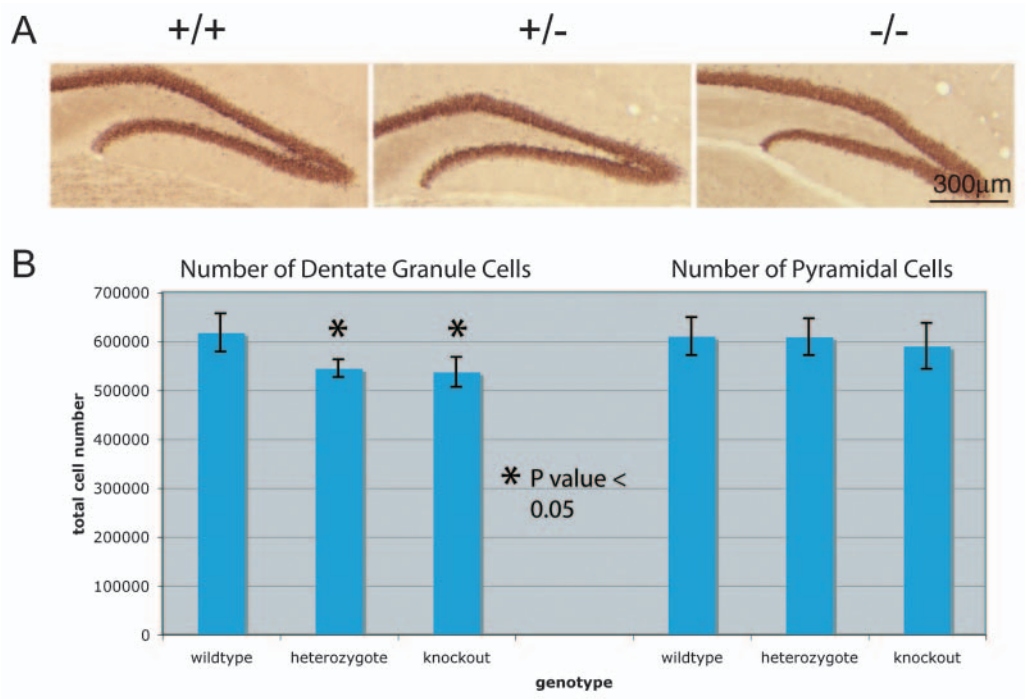

Fig. 3. Stereologic analysis of the adult hippocampus. (A) Prox1 antibody staining of the dentate showing that the overall organization of the dentate is intact in frizzled 9 mutants. (B) Heterozygous and null frizzled 9 mutants have small but statistically significant decreases in the number of dentate granule cells but normal numbers of pyramidal neurons. For each genotype six animals (three male and three female) were used for counting.

such as pentylenetetrazole. This is most readily measured by examining the latency of onset to seizures using defined clinically staging (Tecott et al., 1995). We examined the latency of seizure onset, comparing +/+, +/– and –/– mice of matched age and from the same litters at 10 months of age. This analysis showed a seizure latency of approximately half the time in both the +/– and –/– mice both of which were significantly different than in +/+ mice (Fig. 6A). To determine whether gliosis from excess developmental apoptosis is related to the lowered seizure threshold in mutant mice, we examined GFAP immunohistochemistry and found no differences between the three genotypes (Fig. 6B). This is consistent with the failure to find gliosis in other mouse mutants with excess developmental cell death due to failed trophic support. Although we failed to observe spontaneous seizures in frizzled 9 mutant mice (except for one instance of a handling related seizure in an adult frizzled 9 +/– mouse) it is possible that the lowered seizure threshold is associated with onobserved spontaneous seizures, in which case, one might expect to find mossy fiber sprouting in adult mutants. To address this, we examined Calbindin immunoreactivity in the dentate gyrus of adult mice and found no evidence for abnormal sprouting of the dentate granule cell mossy fiber axon terminals into the dentate molecular layer or CA3 infrapyramidal layer (Fig. 6C).

Frizzled 9 mutant mice show deficits in spatial memory behaviors

As presented above, the frizzled 9 mutant mice displayed alteration of hippocampal cellular composition and lowered seizure thresholds, i.e. abnormality of hippocampal structure and function. Thus, to evaluate this mutation further with regard to hippocampal function and relevance to the spatial processing deficits associated with Williams Syndrome, we tested the hypothesis that frizzled 9 mutant mice would display deficits in visually mediated, spatial memory behaviors. Hippocampal injury or abnormality sustained during early development has been shown to severely disrupt the development of spatial memory behaviors in rodents (Almli et al., 2000; Altemus and Almli, 1997) and the Morris water maze is the most established methodology for examining this function in rodents (Morris, 1984). Starting at 120 days of age, three groups of mice (+/+, +/– and –/– genotypes) were tested in the Morris water maze (Morris, 1984), under the cue (visible platform in fixed location) condition, place (hidden platform in fixed location) condition, and random (hidden platform in random platform location) condition, and the behavioral data were analyzed with analysis of variance and Tukey's HSD or Newman-Keuls post-tests.

We focused on spatial 'memory' behaviors measured during probe (memory) trials for testing under the place (hidden platform in fixed location) condition in the maze. These measures are: probe times (time spent in the maze quadrant that previously contained the platform) and number of annulus crossings (number of times crossing the exact same position/spot where the platform had been previously located) (Fig. 7).

The means (plus standard errors) for two measures of spatial memory during place condition probe trials are presented in Fig. 7 (A=probe time in seconds, B=number of annulus crossings). Inferential statistical analyses of these measures of spatial memory revealed that: (1) the –/– mice displayed significantly shorter probe times during probe/memory trials under the place/spatial condition than the +/+ (P<0.04) or +/– (P<0.03) mice (Fig. 7A); and (2) the –/– mice displayed significantly fewer annulus crossings during probe/memory trials under the place/spatial condition than the +/+ (P<0.004) and +/– (P<0.009) mice (Fig. 7B). For both probe time and annulus crossing measures during the probe (memory) trials under the place/spatial condition, the +/+ mice and +/– mice did not statistically differ from one another (P>0.05). The three groups of mice did not statistically differ (P>0.05) for either

probe times or annulus crossings during the probe/memory trials when tested under either the cue (visible platform in fixed location) or random (hidden platform in random location) testing conditions.

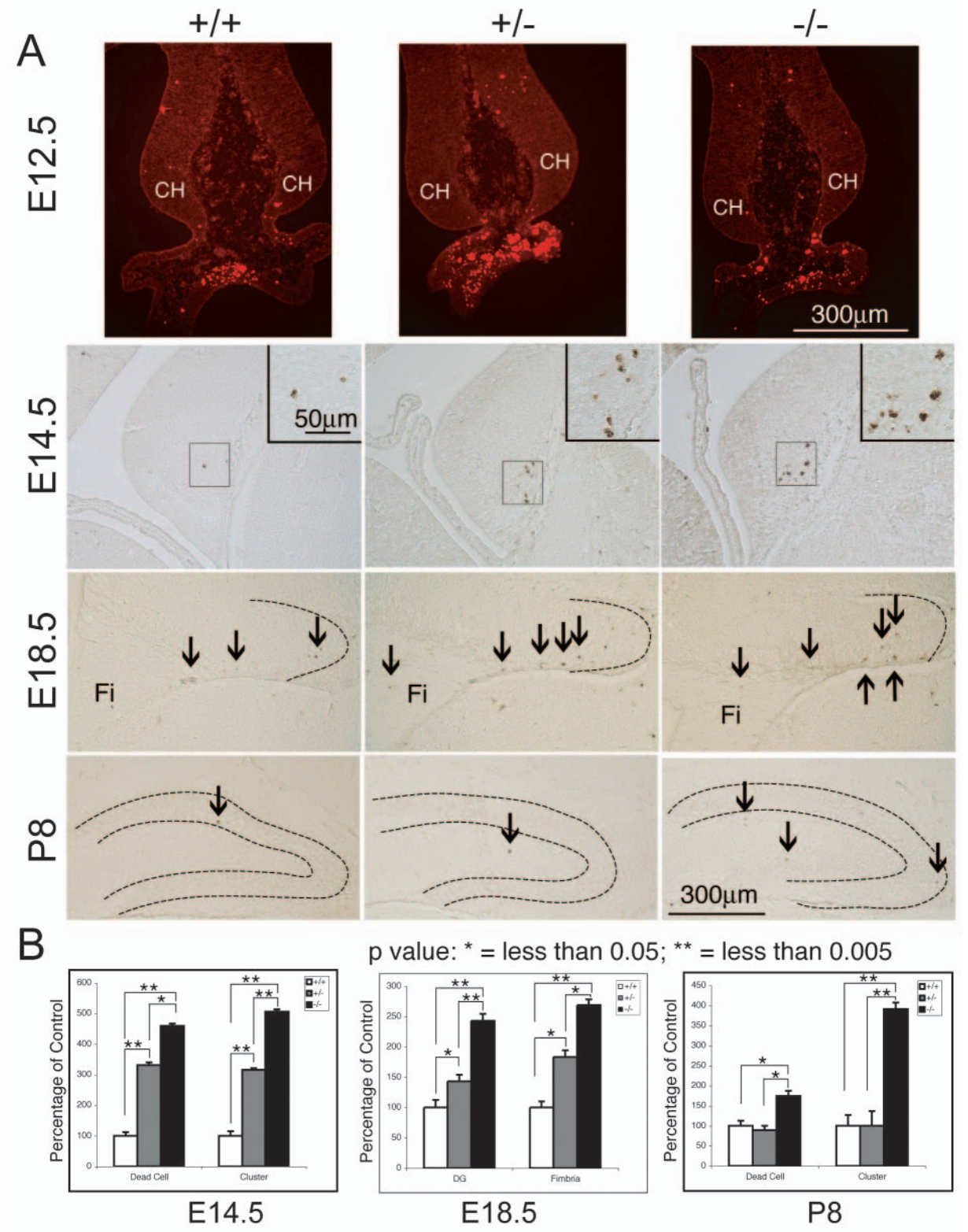

Fig. 4. Increased apoptotic cell death in frizzled 9 mutants. (A) TUNEL staining at E12.5, E14.5, E18.5 and P8 mice. The dotted lines outline the forming dentate gyrus at E18.5 and the dentate granule cell layer at P8. At E12.5, note the numerous labeled cells at the exact midline where the choroid forms but very few cells in the cortical hem (CH) or ventricular zone dorsal to it. (B) Counting of individual labeled cells and clusters of cells expressed at % of wild type. **P*<0.05; ***P*<0.005.

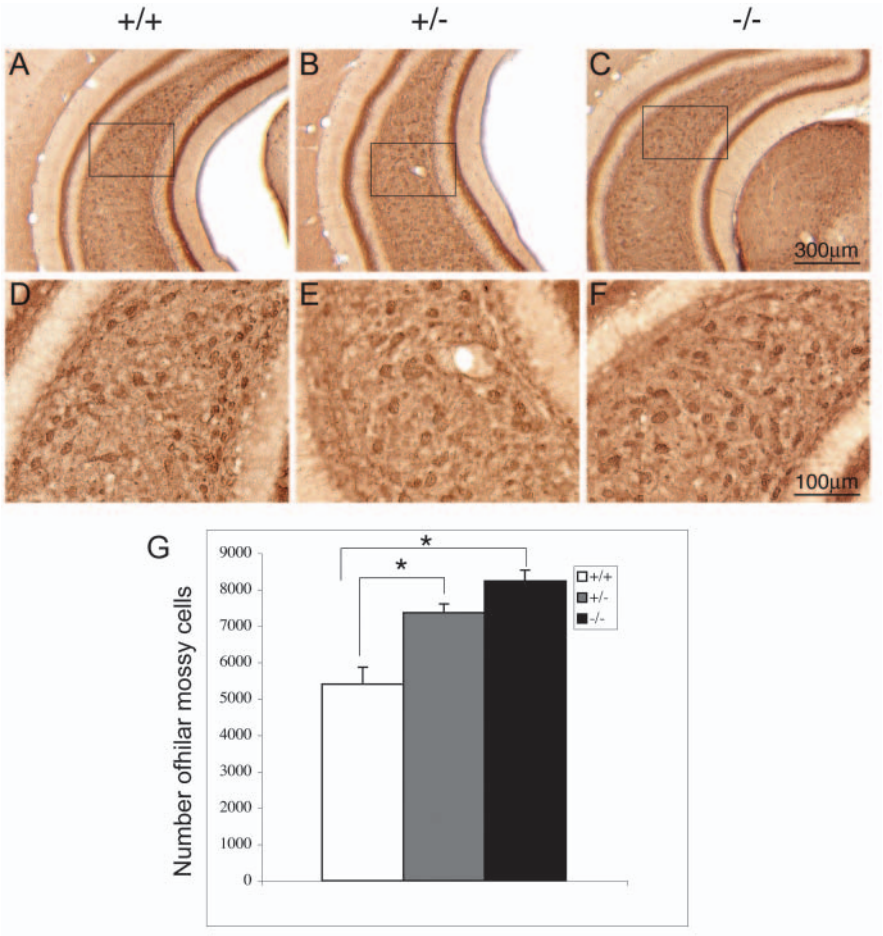

Fig. 5. Increased numbers of hilar mossy cells. (A-F) Calretinin antibody staining shown at low power and high power for all three genotypes. Note the increased density of calretinin labeled cell bodies in the hilus. (G) Quantitation of mossy cell number shows that there is a substantial and significant increase in their numbers in both heterozygous and mutant mice. These cells were counted from the same section series as those used for stereologic analysis. *P<0.05.

These results show that the frizzled 9 mutant (–/–) mice displayed dysfunction of visually mediated, spatial memory processing that persisted well into adulthood. Thus, the spatial memory deficits of the mutant mice may model and reflect the spatial processing deficits associated with Williams Syndrome. It is also interesting that the heterozygous mice tended to be somewhat intermediate between the wild type and mutant mice on the (comparatively crude) measures of spatial memory available for testing rodents. Given the dramatically more complex nature of human cortical processing and interactions between hippocampal structures and associated neocortical areas, it seems quite possible that frizzled 9 heterozygote status in humans would be associated with dramatic cognitive defects.

Discussion

In this study we describe newly generated targeted mutant mice for the Wnt receptor frizzled 9. We targeted frizzled 9 because of its selective expression in the developing hippocampus and because it is within the Williams syndrome deletion interval (the overwhelming majority of Williams syndrome patients are heterozygous for frizzled 9). The mutant mice are viable and fertile but have abnormally high numbers of apoptotic cells in the dentate gyrus and reduction in the total number of granule cells. This appears to be partially counterbalanced by small increases in the numbers of mitotic precursors in the dentate compartment and an increase in the number of mossy cells produced from the adjacent neuroepithelium. For all the neurodevelopmental anatomic defects, the +/– mice are intermediate in severity. Supporting the idea that these anatomic defects are functionally important, the adult mutants have lowered seizure threshold and defects in a hippocampal visuospatial learning task.

Wnts and the control of developmental apoptosis

Our analysis strongly suggests that Wnt signaling may control survival of immature cells in the developing hippocampus along with its well-described role in regulating cellular proliferation. Recent studies have shown similar findings for other morphogenic signaling molecules in the developing CNS. The roles of Sonic Hedgehog as both a developmental morphogen and regulator of proliferation have been widely reported (Ruiz et al., 2002; Marti and Bovolenta, 2002), but recently Patched, the receptor for Sonic Hedgehog, was shown to regulate developmental apoptosis of neural tube precursors (Thibert et al., 2003). Interestingly this effect was blocked by ligand binding to Patched. In this case a morphogenic signal is also required to block programmed cell death in cells expressing the receptor for this molecule. The role of BMP signaling in regulating developmental apoptosis has long been known (Furuta et al., 1997), but recent studies have shown a particular role for BMP signaling in controlling apoptosis required to shape the early development of the medial cortical wall (Hebert et al., 2002; Panchision et al., 2001). In the case of BMPs, the ligands are positive regulators of apoptosis in the medial cortical wall. Our study demonstrates that the loss of a Wnt receptor, selectively expressed in the medial cortical wall, leads to an increase in apoptosis. This implies that a Wnt signal is normally required to inhibit apoptosis in the developing dentate gyrus, perhaps in opposition to BMP effects. At this time we do not know which ligand would be operative in this pathway since there are so many candidate ligands expressed in this region developmentally.

Previous studies have failed to show any evidence of alterations in cell death in the hippocampus of mutants with defects in the canonical Wnt signaling pathway (Lee et al., 2000; Galceran et al., 2000; Zhou et al., 2004). In fact, in these studies loss of Wnt signaling was shown to cause a decrease

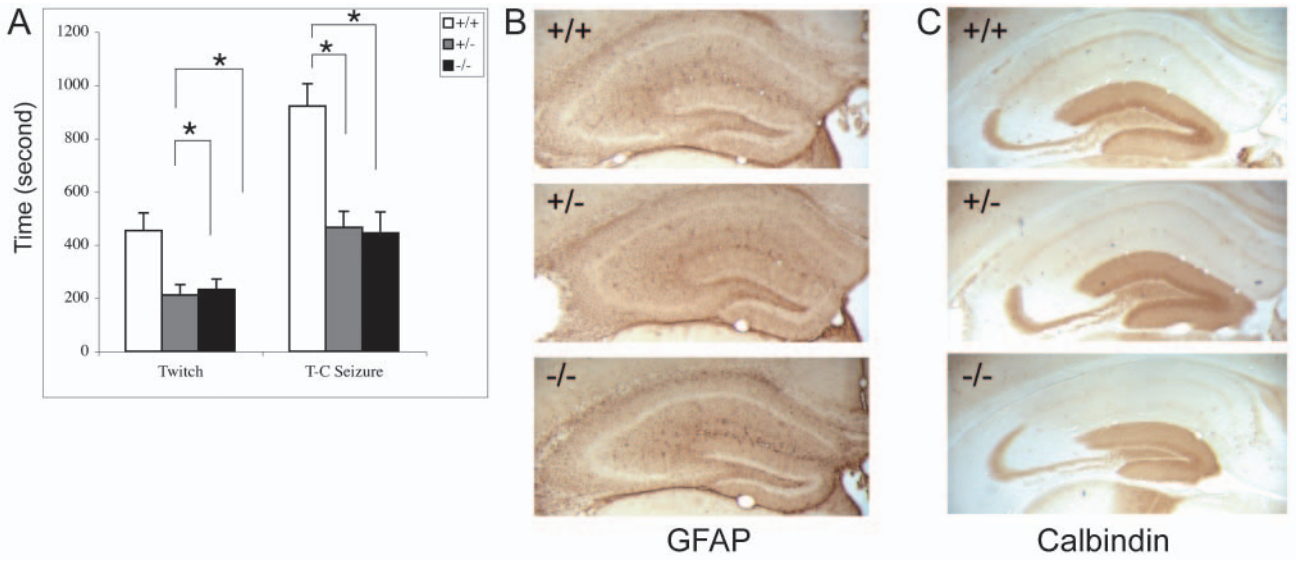

Fig. 6. Seizure latency is decreased in frizzled 9 mutants. (A) Time in seconds to first twitch and to tonic-clonic seizure are shown. The latency of +/– and –/– mice is about half for each endpoint. n=6 for each genotype with 3 females and 3 males of each genotype. *P<0.05. (B) GFAP immunostaining in adult frizzled 9 +/+, +/– and –/– mice. (C) Calbindin immunostaining in adult frizzled 9 +/+, +/– and –/– mice.

in precursor proliferation in the hippocampus and dentate gyrus, an effect quite inconsistent with the results of this study. This raises the very real likelihood that frizzled 9 is active in a non-canonical Wnt signaling pathway (Kuhl et al., 2000; Wallingford et al., 2000). It is still quite possible that frizzled 9 is also active normally in the canonical Wnt pathway but that this function is largely redundant with other frizzled proteins, several of which are expressed in domains overlapping with frizzled 9 (Rattner et al., 1997; Kim et al., 2001). Previous studies have shown that several members of the frizzled family may be active in a variety of Wnt signaling pathways in vertebrates and that this may depend on the specific Wnt ligand they interact with in any given situation (Kuhl et al., 2000).

Our finding of elevated apoptosis in a frizzled mutant is not unprecedented; frizzled 4 mutants have increased apoptosis of cerebellar neurons developing postnatally (Wang et al., 2001). A major question that follows from these studies is how mechanistically frizzleds 4 and 9 regulate survival. Is this via canonical Wnt signaling, non-canonical Wnt signaling or by interactions with entirely separate signaling pathways? A recent study analyzing the role of Wnt signaling in midbrain dopaminergic neuron development showed that three Wnt ligands each regulated dopaminergic neuronal production by affecting the behavior of precursor cells in distinct ways at different stages (Castelo-Branco et al., 2003). In each case, these ligands acted through the canonical Wnt pathway but led to markedly different effects on precursor dynamics and neuronal differentiation. This implies that separate receptor signaling systems might be responsible for these effects all utilizing similar intracellular pathways but acting in different

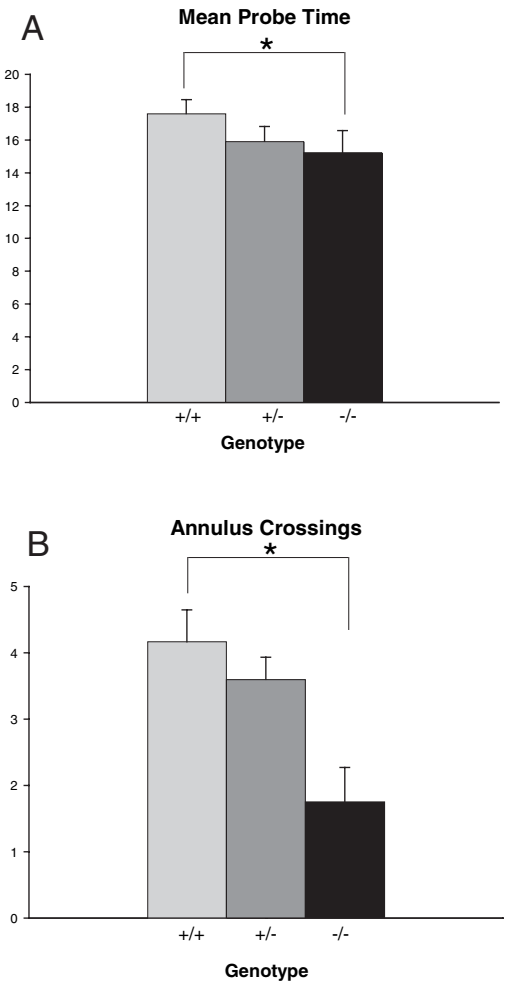

Fig. 7. Measures of spatial memory performance of frizzled 9 mutant mice [+/+ (n=8), +/– (n=12), –/– (n=9)] tested in the Morris water maze (Morris, 1984) under the place/spatial testing condition. Presented are Probe Times in seconds (A) and Number of Annulus Crossings (B) measured during probe trials (i.e. memory trials). The frizzled 9 mutant (–/–) mice displayed significantly (*P<0.04) poorer spatial memory performance on both measures than the +/+ mice, and the +/– mice tended to be intermediate.

ways in distinct cellular contexts. Also of major interest is whether the increase of apoptosis feeds back to regulate precursor proliferation. A recent study in *Drosophila* showed that, in response to developmental apoptosis, there is compensatory activation of the canonical Wnt and JNK pathways leading to increases in proliferation (Ryoo et al., 2004). If a similar mechanism is at play in the frizzled 9 mice, then understanding such mechanisms and harnessing them would potentially allow enhancement of the brains intrinsic abilities to replace sick or dying neurons.

Williams syndrome and frizzled 9

Williams syndrome is a developmental disorder with a number of cognitive and somatic features. The typical deletion interval for Williams syndrome comprises a large number of genes of known and unknown function. Patients with more limited versions of the syndrome and smaller deletions have helped to refine two regions within the deletion interval that are so-called cognitive 'hotspots'. The full-fledged Williams cognitive syndrome presumably requires deletion of both of these regions (Bellugi et al., 1999). Frizzled 9 is contained within one of these 'hotspots' (Bellugi et al., 1999). Initially great interest was shown in the LIMK1 gene that is contained within microdeletions in two families and appeared to be tightly associated with the cognitive symptoms of Williams syndrome (Frangiskakis et al., 1996; Tassabehji et al., 1996), however, further analysis of other patients with microdeletions indicated that deletion of LIMK1 is either unrelated or at most necessary but not sufficient for the cognitive defects in Williams syndrome (Tassabehji et al., 1999). The discrepancy between the initial association of LIMK1 and Williams and the later studies is believed to be due to the highly repetitive nature of this region of Chromosome 7q11.23 leading to the possibility of multiple microdeletions in the same individual (Tassabehji et al., 1999). Thus far, studies of mouse mutants for genes deleted in the typical larger Williams syndrome deletion intervals have implicated CLIP-115 (a microtubule-associated protein) as a potential contributor to the cognitive phenotype (Hoogenraad et al., 2002) but none have fully recapitulated the complex spectrum of Williams syndrome. This has led to the idea that multiple genes may contribute to the cognitive defects (Tassabehji et al., 1999; Hoogenraad et al., 2002). It is in this context that our findings on frizzled 9 mutant mice make it seem quite likely that frizzled 9 is a further contributor to this fascinating syndrome. The strongly visuospatial nature of the defects in Williams syndrome suggests a role for hippocampal circuitry in this disorder and our study sheds important light on the potential role of cytologic abnormalities during dentate gyrus development in this process. Supporting the importance of dentate gyrus anatomic integrity during development on memory function in children is a recent study that showed that developmental defects in hippocampal development have a strong independent association, separable from other brain anomalies, with memory disturbances in older children (Isaacs et al., 2003).

The hippocampal anatomic phenotypes of the frizzled 9 mutants (both +/– and –/– genotypes) are likely to be quite significant for understanding Williams syndrome on a number of levels. As we have shown, frizzled 9 +/– and –/– mutants have reduced latency to onset of seizures in response to a chemoconvulsant. This is likely due to a network imbalance in two important classes of excitatory neurons in the hippocampus that are generally synaptic partners (granule neurons and mossy cells) and is consistent with the fact that about half of patients with Williams syndrome are epileptic (Trauner et al., 1989). Also predicted from our finding that there is a decrease in granule cell number in adult frizzled 9 mutants is the failure of the null mice to perform appropriately on Morris water maze testing. Since this is a test of hippocampal visuospatial learning it is likely to be significant given the selective visuospatial processing defects in Williams syndrome patients.

The authors acknowledge Grant Li, Christine Pozniak, Chengji Zhou, John Rubenstein and Ugo Borello for valuable discussions, Szu-Min Han and Ni-Chi Wu for technical assistance. This work was supported by NIH (NS02208, MH66084), the Burroughs Wellcome Fund, the John Merck Fund, the Whitehall Foundation and the National Alliance for Autism Research to S.J.P. and NS-35902 to C.R.A.

References

Alder, J., Lee, K. J., Jessell, T. M. and Hatten, M. E. (1999). Generation of cerebellar granule neurons in vivo by transplantation of BMP-treated neural progenitor cells. *Nat. Neurosci.* **2**, 535-540.

Almli, C. R., Levy, T. J., Han, B. H., Shah, A. R., Gidday, J. M. and Holtzman, D. M. (2000). BDNF protects against spatial memory deficits following neonatal hypoxia-ischemia. *Exp. Neurol.* **166**, 99-114.

Altemus, K. L. and Almli, C. R. (1997). Neonatal hippocampal damage in rats: long-term spatial memory deficits and associations with magnitude of hippocampal damage. *Hippocampus* **7**, 403-415.

Altman, J. and Das, G. D. (1965a). Post-natal origin of microneurones in the rat brain. *Nature* **207**, 953-956.

Altman, J. and Das, G. D. (1965b). Autoradiographic and histological evidence of postnatal hippocampal neurogenesis in rats. *J. Comp. Neurol.***124**, 319-335.

Bagri, A., Gurney, T., He, X., Zou, Y. R., Littman, D. R., Tessier-Lavigne, M. and Pleasure, S. J. (2002). The chemokine SDF1 regulates migration of dentate granule cells. *Development* **129**, 4249-4260.

Bellugi, U., Lichtenberger, L., Mills, D., Galaburda, A. and Korenberg, J. R. (1999). Bridging cognition, the brain and molecular genetics: evidence from Williams syndrome. *Trends Neurosci.* **22**, 197-207.

Castelo-Branco, G., Wagner, J., Rodriguez, F. J., Kele, J., Sousa, K., Rawal, N., Pasolli, H. A., Fuchs, E., Kitajewski, J. and Arenas, E. (2003). Differential regulation of midbrain dopaminergic neuron development by Wnt-1, Wnt-3a, and Wnt-5a. *Proc. Natl. Acad. Sci. USA* **100**, 12747-12752.

Chenn, A. and Walsh, C. A. (2002). Regulation of cerebral cortical size by control of cell cycle exit in neural precursors. *Science* **297**, 365-369.

Frangiskakis, J. M., Ewart, A. K., Morris, C. A., Mervis, C. B., Bertrand, J., Robinson, B. F., Klein, B. P., Ensing, G. J., Everett, L. A., Green, E. D. et al. (1996). LIM-kinase1 hemizygosity implicated in impaired visuospatial constructive cognition. *Cell* **86**, 59-69.

Furuta, Y., Piston, D. W. and Hogan, B. L. (1997). Bone morphogenetic proteins (BMPs) as regulators of dorsal forebrain development. *Development* **124**, 2203-2212.

Galceran, J., Miyashita-Lin, E. M., Devaney, E., Rubenstein, J. L. and Grosschedl, R. (2000). Hippocampus development and generation of dentate gyrus granule cells is regulated by LEF1. *Development* **127**, 469-482.

Hebert, J. M., Mishina, Y. and McConnell, S. K. (2002). BMP signaling is required locally to pattern the dorsal telencephalic midline. *Neuron* **35**, 1029-1041.

Hoogenraad, C. C., Koekkoek, B., Akhmanova, A., Krugers, H., Dortland, B., Miedema, M., van Alphen, A., Kistler, W. M., Jaegle, M., Koutsourakis, M. et al. (2002). Targeted mutation of Cyln2 in the Williams syndrome critical region links CLIP-115 haploinsufficiency to neurodevelopmental abnormalities in mice. *Nat. Genet.* **32**, 116-127.

Ikeya, M., Lee, S. M., Johnson, J. E., McMahon, A. P. and Takada, S. (1997). Wnt signalling required for expansion of neural crest and CNS progenitors. *Nature* **389**, 966-970.

Isaacs, E. B., Vargha-Khadem, F., Watkins, K. E., Lucas, A., Mishkin, M. and Gadian, D. G. (2003). Developmental amnesia and its relationship to degree of hippocampal atrophy. *Proc. Natl. Acad. Sci. USA* **100**, 13060-13063.

Karasawa, T., Yokokura, H., Kitajewski, J. and Lombroso, P. J. (2002). Frizzled-9 Is Activated by Wnt-2 and Functions in Wnt/beta–Catenin Signaling. *J. Biol. Chem.* **277**, 37479-37486.

Kim, A. S., Lowenstein, D. H. and Pleasure, S. J. (2001). Wnt receptors and Wnt inhibitors are expressed in gradients in the developing telencephalon. *Mech. Dev.* **103**, 167-172.

Kuhl, M., Sheldahl, L. C., Park, M., Miller, J. R. and Moon, R. T. (2000). The Wnt/Ca2+ pathway: a new vertebrate Wnt signaling pathway takes shape. *Trends Genet.* **16**, 279-283.

Lee, S. M., Tole, S., Grove, E. and McMahon, A. P. (2000). A local Wnt-3a signal is required for development of the mammalian hippocampus. *Development* **127**, 457-467.

Marti, E. and Bovolenta, P. (2002). Sonic hedgehog in CNS development: one signal, multiple outputs. *Trends Neurosci.* **25**, 89-96.

Morris, R. (1984). Developments of a water-maze procedure for studying spatial learning in the rat. *J. Neurosci. Meth.* **11**, 47-60.

Muroyama, Y., Fujihara, M., Ikeya, M., Kondoh, H. and Takada, S. (2002). Wnt signaling plays an essential role in neuronal specification of the dorsal spinal cord. *Genes Dev.* **16**, 548-553.

Nowakowski, R. S. and Rakic, P. (1979). The mode of migration of neurons to the hippocampus: a Golgi and electron microscopic analysis in foetal rhesus monkey. *J. Neurocytol.* **8**, 697-718.

Nowakowski, R. S. and Rakic, P. (1981). The site of origin and route and rate of migration of neurons to the hippocampal region of the rhesus monkey. *J. Comp. Neurol.* **196**, 129-154.

Panchision, D. M., Pickel, J. M., Studer, L., Lee, S. H., Turner, P. A., Hazel, T. G. and McKay, R. D. (2001). Sequential actions of BMP receptors control neural precursor cell production and fate. *Genes Dev.* **15**, 2094-2110.

Rattner, A., Hsieh, J. C., Smallwood, P. M., Gilbert, D. J., Copeland, N. G., Jenkins, N. A. and Nathans, J. (1997). A family of secreted proteins contains homology to the cysteine-rich ligand-binding domain of frizzled receptors. *Proc. Natl. Acad. Sci. USA* **94**, 2859-2863.

Ratzliff, A. H., Santhakumar, V., Howard, A. and Soltesz, I. (2002). Mossy cells in epilepsy: rigor mortis or vigor mortis. *Trends Neurosci.* **25**, 140-144.

Ruiz, I. A. A., Palma, V. and Dahmane, N. (2002). Hedgehog-Gli signalling and the growth of the brain. *Nat. Rev. Neurosci.* **3**, 24-33.

Ryoo, D. R., Gorenc, T. and Steller, H. (2004). Apoptotic cells can induce compensatory proliferation through the JNK and the Wingless signaling pathways. *Dev. Cell* **7**, 491-501.

Sloviter, R. S., Zappone, C. A., Harvey, B. D., Bumanglag, A. V., Bender, R. A. and Frotscher, M. (2003). 'Dormant basket cell' hypothesis revisited: relative vulnerabilities of dentate gyrus mossy cells and inhibitory interneurons after hippocampal status epilepticus in the rat. *J. Comp. Neurol.* **459**, 44-76.

Tassabehji, M., Metcalfe, K., Fergusson, W. D., Carette, M. J., Dore, J. K., Donnai, D., Read, A. P., Proschel, C., Gutowski, N. J., Mao, X. et al. (1996). LIM-kinase deleted in Williams syndrome. *Nat. Genet.* **13**, 272-273.

Tassabehji, M., Metcalfe, K., Karmiloff-Smith, A., Carette, M. J., Grant, J., Dennis, N., Reardon, W., Splitt, M., Read, A. P. and Donnai, D. (1999). Williams syndrome: use of chromosomal microdeletions as a tool to dissect cognitive and physical phenotypes. *Am. J. Hum. Gen.* **64**, 118-125.

Tecott, L. H., Sun, L. M., Akana, S. F., Strack, A. M., Lowenstein, D. H., Dallman, M. F. and Julius, D. (1995). Eating disorder and epilepsy in mice lacking 5-HT2c serotonin receptors. *Nature* **374**, 542-546.

Thibert, C., Teillet, M. A., Lapointe, F., Mazelin, L., Le Douarin, N. M. and Mehlen, P. (2003). Inhibition of neuroepithelial patched-induced apoptosis by sonic hedgehog. *Science* **301**, 843-846.

Trauner, D. A., Bellugi, U. and Chase, C. (1989). Neurologic features of Williams and Down syndromes. *Pediatr. Neurol.* **5**, 166-168.

Wallingford, J. B., Rowning, B. A., Vogeli, K. M., Rothbacher, U., Fraser, S. E. and Harland, R. M. (2000). Dishevelled controls cell polarity during Xenopus gastrulation. *Nature* **405**, 81-85.

Wang, Y., Macke, J. P., Abella, B. S., Andreasson, K., Worley, P., Gilbert, D. J., Copeland, N. G., Jenkins, N. A. and Nathans, J. (1996). A large family of putative transmembrane receptors homologous to the product of the Drosophila tissue polarity gene frizzled. *J. Biol. Chem.* **271**, 4468-4476.

Wang, Y., Huso, D., Cahill, H., Ryugo, D. and Nathans, J. (2001). Progressive cerebellar, auditory, and esophageal dysfunction caused by targeted disruption of the frizzled-4 gene. *J. Neurosci.* **21**, 4761-471.

Wang, Y., Thekdi, N., Smallwood, P. M., Macke, J. P. and Nathans, J. (2002). Frizzled-3 is required for the development of major fiber tracts in the rostral CNS. *J. Neurosci.* **22**, 8563-8573.

Wang, Y. K., Samos, C. H., Peoples, R., Perez-Jurado, L. A., Nusse, R. and Francke, U. (1997). A novel human homologue of the Drosophila frizzled wnt receptor gene binds wingless protein and is in the Williams syndrome deletion at 7q11.23. *Hum. Mol. Genet.* **6**, 465-472.

Wang, Y. K., Sporle, R., Paperna, T., Schughart, K. and Francke, U. (1999). Characterization and expression pattern of the frizzled gene Fzd9, the mouse homolog of FZD9 which is deleted in Williams-Beuren syndrome. *Genomics* **57**, 235-248.

West, M. J., Slomianka, L. and Gundersen, H. J. (1991). Unbiased stereological estimation of the total number of neurons in the subdivisions of the rat hippocampus using the optical fractionator. *Anat. Rec.* **231**, 482-497.

Zhao, C. and Pleasure, S. J. (2004). Frizzled-9 promoter drives expression of transgenes in the medial wall of the cortex and its chief derivative the hippocampus. *Genesis* **40**, 32-39.

Zhao, C. and Pleasure, S. J. (2005). Frizzled9 protein is regionally expressed in the developing medial cortical wall and the cells derived from this region. *Dev. Brain Res.* (in press).

Zhou, C. J., Zhao, C. and Pleasure, S. J. (2004). Wnt signaling mutants have decreased dentate granule cell production and radial glial scaffolding abnormalities. *J. Neurosci.* **24**, 121-126.